

1 **Full Title**

2 DiffBrainNet: differential analyses add new insights into the response to glucocorticoids at the level of  
3 genes, networks and brain regions

4 **Short Title**

5 DiffBrainNet: differential networks and expression in 8 mouse brain regions

6

7 Nathalie Gerstner<sup>1,2,3\*</sup>, Anthi C. Krontira<sup>1,2\*</sup>, Cristiana Cruceanu<sup>1</sup>, Simone Roeh<sup>1</sup>, Benno Pütz<sup>1</sup>, Susann

8 Sauer<sup>1</sup>, Monika Rex-Haffner<sup>1</sup>, Mathias V. Schmidt<sup>4</sup>, Elisabeth B. Binder<sup>1\*#</sup>, Janine Knauer-Arloth<sup>1,3\*#</sup>

9 \*authors contributed equally

10 #co-corresponding authors

11 Elisabeth B. Binder: [binder@psych.mpg.de](mailto:binder@psych.mpg.de)

12 Janine Knauer-Arloth: [arloth@psych.mpg.de](mailto:arloth@psych.mpg.de)

13

14 1. Department of Translational Research in Psychiatry, Max Planck Institute of Psychiatry,  
15 Munich, Germany

16 2. International Max Planck Research School for Translational Psychiatry, Munich, Germany

17 3. Institute of Computational Biology, Helmholtz Zentrum München, Neuherberg, Germany

18 4. Research Group Neurobiology of Stress Resilience, Max Planck Institute of Psychiatry, Munich,  
19 Germany

20

21

22

23

24

25

26

27 **Abstract**

28 Genome-wide gene expression analyses are invaluable tools for increasing our knowledge of biological  
29 and disease processes, allowing a hypothesis-free comparison of gene expression profiles across  
30 experimental groups, tissues and cell types. Traditionally, transcriptomic data analysis has focused on  
31 gene-level effects found by differential expression. In recent years, network analysis has emerged as  
32 an important additional level of investigation, providing information on molecular connectivity,  
33 especially for diseases associated with a large number of linked effects of smaller magnitude, like  
34 neuropsychiatric disorders and their risk factors, including stress. In this manuscript, we describe how  
35 combined differential expression and prior-knowledge-based differential network analysis can be  
36 used to explore complex datasets. As an example, we analyze the transcriptional responses following  
37 administration of the glucocorticoid/stress hormone receptor agonist dexamethasone in *C57Bl/6*  
38 mice, in 8 brain regions important for stress processing: the prefrontal cortex, the amygdala, the  
39 paraventricular nucleus of the hypothalamus, the cerebellar cortex, and sub regions of the  
40 hippocampus: the dorsal and ventral *Cornu Ammonis 1*, the dorsal and ventral dentate gyrus. By  
41 applying a combination of differential network- and differential expression- analyses, we find that  
42 these explain distinct but complementary aspects and biological mechanisms of the responses to the  
43 stimulus. In addition, network analysis identifies new differentially connected partners of important  
44 genes and can be used to generate hypotheses on specific molecular pathways affected. With this  
45 work, we provide an analysis framework and a publicly available resource for the study of the  
46 transcriptional landscape of the mouse brain: DiffBrainNet (<http://diffbrainnet.psych.mpg.de>), which  
47 can identify molecular pathways important for basic functioning and response to glucocorticoids in a  
48 brain-region specific manner.

49

50

51

52

## 53 Introduction

54 High-throughput transcriptomics are extensively employed to study healthy as well as disease-related  
55 tissue expression profiles from *in vitro* and *in vivo* model systems or human tissue. Traditionally,  
56 transcriptomic data analysis has been based on differential expression (DE) analysis and has focused  
57 on gene-level associations to phenotypes. In the last decade, gene set enrichment analysis [1] and  
58 network analysis [2–4] have emerged allowing the study of complex associations between sets of  
59 genes, in multiple tissues and for multiple outcomes [5,6,15–17,7–14].

60 Network analysis is critical for the study of relationships between genes, and in turn, of molecular  
61 pathways. This is especially true for complex disorders for which risk is conferred by a combination of  
62 many small effects. Strong DE can be expected with major genetic or environmental impacts such as  
63 in cancer [18,19]. For other disorders, for example in neuropsychiatry, risk is driven by multiple  
64 polygenic and interlaced environmental factors that affect a multitude of transcripts, often with only  
65 small effect sizes [20,21]. A combinatorial analysis framework of DE and network analysis has proven  
66 very useful for unraveling additional biology and pathomechanisms of complex disorders [5]. For  
67 example, gene co-expression networks, based on Pearson correlations, along with DE analysis have  
68 been used to study shared and distinct transcriptomic profiles of five major neuropsychiatric disorders  
69 (autism spectrum disorder; schizophrenia, bipolar disorder, major depressive disorder and alcoholism)  
70 leading to the identification of gene modules associated with specific cell-types and disorders [22].

71 Besides correlation-based methods, which tend to suffer from over-connectivity and low specificity,  
72 several other classes of algorithms are used for network inference [23]. More advanced are, for  
73 example, regression-based or Bayesian methods. While Bayesian methods perform poorly on large  
74 datasets and are more suitable for small networks [23], regression- and other machine learning-based  
75 algorithms require large amounts of samples to confidently infer connections in a high-dimensional  
76 input space. To overcome this limitation of regression-based network inference and increase the  
77 performance on datasets with small amounts of samples, the input space can be reduced by  
78 facilitating prior-knowledge [24]. Prior-knowledge refers to already described functional relationships

79 between transcripts or proteins, accessible from publicly available databases. The Knowledge guided  
80 Multi-Omics Network inference approach (KiMONo) implements such a combination of prior-guided  
81 regression-based network inference and was previously shown to be a powerful approach to infer  
82 integrated multi-level networks [3].

83 Traditionally the stimulus or disease impact on networks has been modeled by associating modules of  
84 co-expressed genes with disease phenotypes or comparing the number of connections a gene has in  
85 the control and stimulus networks. This has proven challenging given that it is based on the  
86 comparison of networks with different topological characteristics [4]. To tackle this, differential  
87 network (DN) analysis has emerged. DN analysis computes the differential co-expression and  
88 regulatory interactions of many genes in a single network and analyzes biological processes inferred  
89 from one DN [25], thus eliminating the problems arising when trying to compare two or more  
90 networks at different stimulation paradigms. DN analysis offers the possibility to study the directed  
91 multivariate effects of the treatment or disease state on the genes' neighborhoods. Another  
92 advantage of using prior-knowledge network analysis algorithms is that the inferred networks have  
93 the same topological characteristics which results in a more robust calculation of the differential  
94 connections.

95 In this study, we now leverage the power of DN approaches and calculate regression- and prior-  
96 knowledge-based genome-wide networks from RNA expression data of 8 mouse brain regions  
97 following a vehicle or a pharmacological stimulus, and compute differential networks in addition to  
98 differential expression. As a stimulus we used dexamethasone, a synthetic glucocorticoid that is a  
99 preferential agonist of the glucocorticoid receptor (GR). GR is a transcription factor able to elicit a  
100 robust transcriptomic response when bound to its agonists [26], it is an important component of the  
101 stress-axis and has been implicated in risk for stress-related psychiatric disorders [27]. The 8 brain  
102 regions were selected for their implication with the activation of the stress axis and the response to  
103 stress, and include a detailed segmentation of the hippocampal formation (ventral and dorsal  
104 dissections of both *Cornu Ammonis 1*- CA1 and dentate gyrus- DG), the prefrontal cortex (PFC), the

105 amygdala (AMY), the cerebellar cortex (CER) and the paraventricular nucleus of the hypothalamus  
106 (PVN). We combined DN with DE analysis in order to provide an analysis framework for transcriptomic  
107 data and a resource of all levels of information. This public resource is named DiffBrainNet  
108 (DiffBrainNet access: <http://diffbrainnet.psych.mpg.de>). We provide examples of how DiffBrainNet  
109 can be used to study the molecular landscape of the brain and unravel biological mechanisms of  
110 response to dexamethasone and GR activation in a brain region-specific manner.

111

## 112 **Materials and Methods**

### 113 Experimental animals

114 All experiments and protocols were performed in accordance with the European Communities' Council  
115 Directive 2010/63/EU and were approved by the committee for the Care and Use of Laboratory  
116 animals of the Government of Upper Bavaria. All mice were obtained from the in-house breeding  
117 facility of the Max Planck Institute of Psychiatry and kept in group housed conditions in individually  
118 ventilated cages (IVC; 30cm x 16 cm x 16 cm; 501 cm<sup>2</sup>) serviced by a central airflow system (Tecniplast,  
119 IVC Green Line – GM500). Animals had ad libitum access to water (tap water) and standard chow and  
120 were maintained under constant environmental conditions (12:12 hr light/dark cycle, 23 ± 2 °C and  
121 humidity of 55%). All IVCs had sufficient bedding and nesting material as well as a wooden tunnel for  
122 environmental enrichment. Animals were allocated to experimental groups in a semi-randomized  
123 fashion, data analysis and execution of experiments were performed blinded to group allocation.

124 3-months old C57Bl/6n male mice (n=15 animals per condition) were injected intraperitoneally with  
125 dexamethasone at a dose of 10 mg/kg body weight (treatment) or 0.9% saline as control (vehicle).  
126 Four hours later the mice were sacrificed, the brain was perfused with a solution of Heparin in 0.9%  
127 saline, extracted and snap-frozen in butanol on dry ice and kept in -80°C until further use. The brains  
128 were cut in 250µm coronal slices and 8 brain regions were isolated following the stereotaxic  
129 coordinates of the mouse brain atlas [28]. In detail, the following brain regions were isolated: cingulate  
130 cortex 1 and 2 (bregma 2.34 to -0.22), from now on referred-to as prefrontal cortex (PFC);

131 paraventricular nucleus of the hypothalamus (PVN; bregma -0.58 to -1.22); amygdala (AMY; bregma  
132 0.02 to -0.94); dorsal Cornu Ammonis 1 (dCA1; bregma -1.22 to -2.80); ventral Cornu Ammonis 1  
133 (vCA1; bregma -2.92 to -3.88); dorsal dentate gyrus (dDG; bregma -0.94 to -2.80), ventral dentate  
134 gyrus (vDG; bregma -2.92 to -3.88) and cerebellar cortex (CER; bregma -5.80 to -6.24). Brain punches  
135 were kept in dry ice while cutting and then in -80oC until the RNA extraction was performed.

136

#### 137 RNA extraction

138 RNA was extracted using an automated Chemagic 360° instrument with an integrated dispenser and  
139 the chemagic RNA Tissue Kit (CMG-1212) following manufacturer's instructions. In short, Chemagic  
140 360° RNA extraction is based on the use of magnetic beads that bind the nucleic acids which are then  
141 isolated using magnetized metal rods. Homogenization of the tissue was achieved using rotating  
142 zirconium beads. Washing steps and subsequent elution of the RNA was achieved by switching off the  
143 magnet while the rods continue to rotate in a buffer of preference. DNA was digested using DNase I  
144 and proteins using Proteinase K. RNA concentration was measured using a Nanodrop and the quality  
145 was measured using TapeStation RNA ScreenTapes (High Sensitivity RNA ScreenTapes, Cat No. 5067-  
146 5579).

147

#### 148 RNA sequencing

149 3' tag RNA sequencing libraries were prepared using the QuantSeq 3' mRNA Fwd kit (Lexogen)  
150 following manufacturer's instructions with the addition of unique molecular identifiers (UMIs- UMI  
151 Second Strand Synthesis Module for QuantSeq FWD) for the tagging of individual transcripts. Libraries  
152 were single-end sequenced on an Illumina HiSeq4000 sequencer using 75bp long reads for a total  
153 coverage of an average of 10M reads per library. Five samples were excluded from sequencing and/  
154 or further analysis due to technical issues with the library preparation: two dexamethasone-treated  
155 dCA1 samples, one dexamethasone-treated PFC sample, one control PVN sample and one control  
156 vCA1 sample.

157 RNA sequencing analysis

158 The quality of sequencing data was analyzed with FastQC v0.11.4 [29] and adapter trimming was  
159 performed with cutadapt v1.11 [30]. Unique molecular identifiers were extracted with UMI-tools  
160 v.0.5.4 [31], before the reads were aligned with the mouse reference genome (mm10, Ensembl release  
161 84) using STAR v2.6.0a [32]. Afterwards, reads were deduplicated with UMI-tools and gene expression  
162 was quantified with featureCounts v1.6.4 [33]. The subsequent analysis was performed in R version  
163 4.0.5 [34]. All genes that were not detected in at least one full treatment group were removed from  
164 the dataset leaving 12,976 genes. Subsequently, genes with less than 10 counts across all samples  
165 within each brain region were excluded (detailed numbers of genes per brain region in Table S1). To  
166 identify outliers, we performed a principal component analysis (PCA) on the samples of each brain  
167 region and treatment group separately. Samples with a distance of more than 2.5 standard deviations  
168 from the mean in the first principle component were excluded (numbers of outliers per brain region  
169 and treatment group in Table S1). Surrogate variable analysis (SVA)[35] was applied to account for  
170 unwanted variation in the data.

171

172 Differential expression (DE) analysis

173 Significant surrogate variables (exact numbers in Table S1) were included as covariates in the DE  
174 analysis. The expression data was normalized and transformed using the vst function of DESeq2  
175 v1.30.1 [36] for SVA and subsequent network analysis. DE analysis between the two treatment groups  
176 was performed for each brain region individually. We tested for DE with DESeq2 using the Wald test  
177 and reported the genes with a false discovery rate (FDR) below 10% as significant.

178

179 DiffBrainNet

180 *Network inference*

181 Networks were generated for vehicle- (referred-to as "vehicle") and dexamethasone-treated  
182 (referred-to as "treatment") samples separately for each brain region using the network inference

183 method: KiMONo [3]. KiMONo uses prior information from existing biological databases that provide  
184 the edges among the transcripts, as a basic network layout. Different omic layers (here only  
185 transcriptomic data) are then used on top of the prior basic-network layout to fit the edge weights in  
186 the network. Edge weights can thereby take on a value smaller than a predefined threshold which  
187 leads to the removal of the edge from the network (Fig 1). More specifically, KiMONo uses a  
188 multivariate regression approach with sparse group lasso penalization to model the expression levels  
189 of the transcripts. The possible predictors in the regression model are inferred from the gene's  
190 connections in a prior network. In the inferred directed gene expression networks, the nodes  
191 represent transcripts of the input data and the edge weights are the beta coefficients ( $\beta$ -value) fitted  
192 by the regression approach (S1B Fig). A  $\beta$ -value  $> 0$  indicates that two genes' expression levels are  
193 correlated positively, while a  $\beta$ -value  $< 0$  indicates that two genes' expression levels are correlated  
194 negatively. Significant surrogate variables identified during DE analysis were used as covariates for  
195 network inference and treated as a separate group in the regression penalization (Table S1). The  $r^2$   
196 value assigned to each regression model is used as a confidence score to indicate the goodness of fit  
197 of the model. In the vehicle and treatment networks, all interactions with an absolute  $\beta$ -value  $< 0.01$   
198 or an  $r^2$  value  $< 0.1$  and the connections to the surrogate variables were excluded.

199 As a prior network we used FunCoup 5 [37], a database which contains about 6.7 million interactions  
200 between 19,771 genes in the mouse organism and that is provided as a framework to infer genome-  
201 wide functional couplings based on data of 10 different evidence types: physical protein interactions,  
202 mRNA co-expression, protein co-expression (based on the human protein atlas), genetic interaction  
203 profile similarities, shared regulation by transcription factor binding, shared regulation by miRNA  
204 targeting, subcellular colocalization, domain interactions, phylogenetic profile similarity, quantitative  
205 mass spectrometry data and gene regulatory data inferred from transcription factor bindings.  
206 FunCoup provides the edges of the basic network layout and KiMONo computes the weights of these  
207 edges fitted from the expression of the transcripts in each brain region and treatment paradigm.

208



## 209 *Differential network analysis*

210 A differential network (DN) for each brain region was calculated by combining the vehicle and  
211 treatment network using the DiffGRN approach [25] which describes differential relationships  
212 between two genes. Thereby, differential gene interactions were calculated from the regression's  $\beta$ -  
213 values and their standard errors using a z-test:

$$214 \quad z_{XY} = \frac{\beta_{XY}^T - \beta_{XY}^V}{\sqrt{SE(\beta_{XY}^T)^2 + SE(\beta_{XY}^V)^2}}$$

215 where  $\beta_{xy}^T$  and  $\beta_{xy}^V$  are the  $\beta$ -values of genes X and Y in the treatment and vehicle networks,  
216 respectively. A z-value  $> 0$  indicates either a stronger positive correlation ( $0 < \beta_{xy}^V < \beta_{xy}^T$ ), a weaker  
217 negative correlation ( $\beta_{xy}^V < \beta_{xy}^T < 0$ ) or a switch from negative to positive correlation ( $\beta_{xy}^V < 0 < \beta_{xy}^T$ )  
218 between genes X and Y from vehicle to treatment network. A z-value  $< 0$  indicates a stronger negative  
219 correlation ( $\beta_{xy}^T < \beta_{xy}^V < 0$ ), a weaker positive correlation ( $0 < \beta_{xy}^T < \beta_{xy}^V$ ) or a switch from positive to  
220 negative correlation ( $\beta_{xy}^T < 0 < \beta_{xy}^V$ ) between genes X and Y from vehicle to treatment network. Z-  
221 values  $> 0$  can be described as relative changes in gene expression leading to a more positive  
222 correlation (termed positive regulatory effect), while z-values  $< 0$  can be described as relative changes  
223 in gene expression leading to a more negative correlation (termed negative regulatory effect) (S1B  
224 Fig). Differential interactions with an FDR adjusted p-value  $\geq 0.01$  associated with the z-score were  
225 excluded.

226

## 227 *Hub gene analysis*

228 We defined key regulators in the vehicle, treatment and differential networks, termed vehicle-,  
229 treatment- and differential- hub genes accordingly. The measure that we used to identify these key  
230 genes was the node-betweenness implemented in the igraph package, which describes the number  
231 of shortest paths going through a node [38]. Since we build the networks on top of a prior network,  
232 the node-betweenness in the networks (vehicle, treatment, differential) is driven by the prior network.  
233 We therefore normalized the node-betweenness as follows,

$$234 \quad \text{node-betweennessNorm}_{\text{networkA}}(\text{gene } X) = \frac{\text{node-betweenness}_{\text{networkA}}(\text{gene } X)}{\text{node-betweenness}_{\text{networkPrior}}(\text{gene } X)}$$

235 where  $\text{node-betweenness}_{\text{networkA}}(\text{gene } X)$  is the node-betweenness of gene X in network A (e.g. DN of  
236 one brain region) and  $\text{node-betweenness}_{\text{networkPrior}}(\text{gene } X)$  is the node-betweenness of the same gene  
237 X in the prior network. We defined all genes with a node-betweenness greater than 10,000 and a  
238 normalized node-betweenness greater than 1.0 as hub genes and compared them between brain  
239 regions as well as with the DE genes identified in the DE analysis.

240

#### 241 Gene set enrichment analysis

242 Enrichment of DE genes or differential hub genes was performed using FUMA GENE2FUNC [39]  
243 analysis based on Gene Ontology (GO, [40,41]), KEGG [42–44], Reactome [45] and genes carrying  
244 single nucleotide polymorphisms (SNPs) with genome-wide association to a variety of traits (analysis  
245 references the NHGRI-EBI GWAS Catalog [46] (<https://www.ebi.ac.uk/gwas/>) most recently updated  
246 on 18 September 2021). Default parameters were used in FUMA, with all genes expressed above  
247 threshold in all brain regions (n=12,830 genes) as the background list. To account for differentially  
248 sized input gene lists, only terms with at least 10% (unless stated otherwise) of the input genes  
249 overlapping with the term genes were considered and p-values were corrected using the Benjamini-  
250 Hochberg (FDR) method [47] to account for multiple comparisons. We used an FDR cut off of 5% for  
251 statistical significance.

252

#### 253 Shiny app

254 To make these data and analyzes searchable by all interested scientists, we created DiffBrainNet,  
255 which is accessible online at <http://diffbrainnet.psych.mpg.de>. The app was written in R (v4.0.5) [34],  
256 uses the shiny package (v1.7.1) [48] and several additional freely available packages (org.Mm.eg.db  
257 v3.14.0, shinythemes v1.2.0, ggplot2 v3.3.5, plotly v4.10.0, visNetwork v2.1.0, data.table v1.14.2,  
258 dplyr v1.0.7, stringr 1.4.0) and is hosted with ShinyProxy[49]. The source code of the app is available

259 via github <https://github.molgen.mpg.de/mpip/DiffBrainNet>. The app can also be run locally using a  
260 docker image available on Docker Hub <https://hub.docker.com/r/ngerst/diffbrainnet>.

261

## 262 **Results**

263 DiffBrainNet: a brain-region specific resource and analysis framework for transcriptomic responses to  
264 glucocorticoid receptor activation

265 In this work, we set out to provide a resource of brain-region-specific transcriptome analyses at the  
266 gene- and network- level exploring the effects of a 4-hour 10mg/kg dexamethasone administration in  
267 8 different mouse brain regions (Fig 1 top and S1A Fig). We used RNA sequencing to measure gene  
268 expression across the whole transcriptome and detected 12,976 genes across the 8 brain regions  
269 (exact numbers of transcripts per brain region in Table S1), with 12,830 genes being common across  
270 all 8 brain regions (Table S2).

271 Network analysis unravels the effects of relative gene expression changes that may not be detected  
272 at the individual DE genes. Therefore, gene expression networks for each condition per brain region  
273 were calculated with regression analysis based on a prior network using KiMONo [3]. As a prior  
274 network we used FunCoup 5.0 [37] which contains experimental data on about 6.7 million interactions  
275 between 19,771 mouse genes, of which 11,083 genes were also detectable in our dataset (5.4 million  
276 interactions). We inferred a DN per brain region by comparing the  $\beta$ -values of the regression analysis  
277 between the vehicle and treatment networks with a z-test, following the DiffGRN [25] approach. In  
278 addition, we also performed differential expression (DE) analysis to assess the gene-level responses  
279 to glucocorticoid receptor activation between vehicle and treatment (Fig 1 middle).

280 To examine if the DE genes are also the ones with the highest co-regulatory responses in the DNs we  
281 identified differential hub genes, i.e. genes with normalized node-betweenness above 1 (Fig 1  
282 bottom). Furthermore, to identify pathways that are regulated by DE genes and/or differential hub  
283 genes we used enrichment analyses of GO terms, KEGG and Reactome pathways and GWAS significant

284 genes. By applying this analysis framework, we were able to compare the transcriptomic responses  
285 across 8 brain regions on multiple complementary levels.

286 All data can be explored in an interactive online resource, called DiffBrainNet  
287 (<http://diffbrainnet.psych.mpg.de>). In the following, we illustrate results obtained from analyses using  
288 DiffBrainNet.

289

### 290 Differential network analysis provides biological information beyond single gene-level analysis

291 We used our framework of combined DE and DN analysis to study the transcriptomic responses to  
292 glucocorticoids (GCs) across the eight brain regions in DiffBrainNet. Principal component (PC) analysis  
293 of the gene expression data showed that PC1 and PC2 explain 62% of the variance. The brain regions  
294 are separated by PC1 and PC2 whereas samples of the same brain region are comparable with respect  
295 to the first two PCs (Fig 2A). Treatment conditions were separated by PC4 and PC5 when PC analysis  
296 was applied on the samples of all brain regions together (Fig 2B). Over all 8 brain regions, we observed  
297 2,092 DE genes (FDR adjusted p-value < 0.1) following dexamethasone administration of which 172  
298 were shared DE across all brain regions (Fig 2C, Table S3). The majority of DE genes of each brain region  
299 were regulated in more than one region and only the minority (5.4-26.6%) was specific to a single  
300 brain region (S2A Fig, Tables S4-S11). The upregulated shared DE genes across all brain regions (N=129)  
301 were significantly enriched for biological processes related to cell death, response to stimulus, signal  
302 transduction and cell proliferation, whereas the downregulated ones (N=43) were enriched for  
303 developmental terms such as neurogenesis, cell differentiation and tissue morphogenesis (S2B Fig,  
304 Table S12).

305 In addition to DE analysis we performed DN analysis across the 8 brain regions and compared numbers  
306 and enrichment patterns of differential hub genes. We observed a total of 755 differential hub genes.  
307 The majority (over 73%) of these differential hub genes were shared between at least 2 brain regions  
308 (Fig 2D and S2C, Tables S13-S20), however, there were 7 differential hub genes shared across all

309 investigated brain regions (*Sox5*, *Lpar1*, *Thy1*, *Mcam*, *Nell2*, *Rab3c*, *Zic1*) (Fig 2D and S2D, Table S21  
310 and S22). Of all the 755 differential hub genes, only 174 were also DE genes in any brain region.  
311 To further explore how DE genes and differential hub genes may relate to different biology, we  
312 compared the unique sets of these genes for the PFC, which was the brain region with the largest  
313 fraction of unique DE genes (n=920 total DE genes of which 245 (26.6%) were unique to PFC, Fig 2C,  
314 Table S11). PFC, together with AMY, was also the brain region with the highest fraction of unique  
315 differential hub genes (n=293 total differential hub genes of which 29 (9.9%) were unique in PFC, Fig  
316 2D, Table S13). None of these 29 unique differential hub genes was also a DE gene in the PFC. A GO  
317 enrichment analysis on the unique DE and unique differential hub genes of the PFC respectively  
318 indicated that the biological functions related to these two sets of genes are distinct (Tables S23 and  
319 S24). While the biological processes with the highest enrichment for unique DE genes were mostly  
320 related to development and signaling (Fig 2E), the top terms for the unique differential hub genes  
321 were mainly global terms related to response to stress or stimulus (Fig 2F; n=14 terms). This suggests  
322 that DE and DN analyses reveal different but complementary information about the transcriptional  
323 response to the stimulus.  
324 To show the added value of DN analysis we focused on *Abcd1*, a member of the ABC protein family  
325 known to actively transport GCs [50,51]. *Abcd1* is the unique differential hub gene that has by far the  
326 highest normalized node-betweenness in the PFC (normalized node-betweenness = 5,829, second  
327 highest is 4,013 for *Slc39a3*, Table S13) and many differential correlations, though it is not a PFC DE  
328 gene (FDR= 0.935; Fig 3A). However, in its DN there are 4 PFC DE genes (FDR < 0.1) and 7 genes that  
329 have a nominal DE p-value < 0.05 (Fig 3B, Table S25). By focusing at the pathways level, enrichment  
330 analyses of the DN of *Abcd1* supports a more general role of ABC transporters in the response to GCs  
331 (Fig 3C and D, Table S26). In addition, *Abcd1* is directly or indirectly connected to two other differential  
332 hub genes, *Tm7sf2* and *Pex5l*, suggesting that it is related to large interconnected DNs (Fig 3B). These  
333 smaller changes in the expression of genes that have in common their connectivity with *Abcd1*  
334 culminate in this gene's status as a differential hub gene above the significance threshold, in spite of

335 its too-subtle change at the individual expression level. Since biologically it is established that no gene  
336 works independently within a cell, these findings highlight the added value of network analysis to  
337 unravel distinct but complementary aspects of transcriptomic responses that can lead to specific  
338 molecular pathways identification.

339

#### 340 Differential network analysis supports the biological understanding of differentially expressed genes

341 Our next aim was to utilize DN to add an extra layer of interpretation to DE results, especially when  
342 the number of DE genes is insufficient for direct pathway analysis, indicating that the individual gene-  
343 level effects are very small. The vCA1 region of the hippocampus had the least number of unique DE  
344 genes from all brain regions with only 5.4% (n=25) of the total vCA1 DEGs (n=466) being unique to this  
345 region (Fig 2C and 4A and Table S8). Enrichment analysis at the GO level did not yield enriched terms  
346 (S3 Fig, FDR < 0.05 and Table S27). We next used these 25 unique DE genes as seeds in DiffBrainNet  
347 and found their differential neighbors, resulting in a DN containing 745 nodes, the 25 unique vCA1 DE  
348 genes and 720 differential neighbors (Table S28). This DN was enriched for genes associated via GWAS  
349 with autism spectrum disorder and depleted from genes associated with schizophrenia and general  
350 cognitive ability (Fig 4B and Table S29). These genes were now significantly enriched for GO terms  
351 associated with nervous system processes, cell morphogenesis, ion transport and synaptic signaling  
352 (Fig 4C and Table S30). This indicates that very small effects on multiple genes resulted in altered  
353 molecular connectivity in vCA1. This was not detected at the gene-level with DE analysis, but it was  
354 detected at the network-level with DN analysis.

355 We next focused on the top enriched GO term based on the gene ratio, "regulation of trans-synaptic  
356 signaling" (FDR =  $8.71 \times 10^{-22}$ ), and visualized the genes that were both part of the vCA1 DE genes  
357 network and associated with this term (Fig 4D). At the center of this DN was *Grm4*, which encodes a  
358 metabotropic glutamate receptor. *Grm4* showed many differential connections to other differential  
359 hub and DE genes including *Cacna1a*, which encodes a subunit of voltage-dependent calcium channels  
360 important for communication between neurons and synaptic signaling [52]. This trans-synaptic

361 signaling network responded to dexamethasone by a number of changed correlations including  
362 several differential hub genes, beyond *Grm4* and *Cacna1a*, namely *Cspg5*, *Brsk1*, *Nlgn3*, *Rab3a* and  
363 *Grin2b*. This combination of DE and DN analysis was instrumental to identify potential biological  
364 responses to dexamethasone in the vCA1 region that were not readily detectable through DE analysis  
365 alone.

366

### 367 DiffBrainNet can support exploring network changes related to candidate genes

368 We next sought to use our resource and analytical framework to investigate biological processes and  
369 pathways regulated by genes previously associated with risk for psychiatric disorders. DiffBrainNet  
370 provides the opportunity to study how genes of interest are co-regulated in different brain regions at  
371 vehicle-treated and after a stimulus, in this case glucocorticoid exposure. Here, we focused on  
372 understanding which biological processes were co-regulated by *Tcf4* (*Transcription factor 4*), a gene  
373 encoding a transcription factor with genome-wide significant associations to a number of different  
374 psychiatric disorders including schizophrenia, major depressive disorder and autism spectrum  
375 disorders [53] and for which mutations have been shown to cause neurodevelopmental disorders like  
376 for example Pitt-Hopkins syndrome [54].

377 We used DiffBrainNet to better understand this interaction by investigating the biological pathways  
378 co-regulated by *Tcf4* in the DNs reflecting changes associated with GR activation. *Tcf4* showed  
379 significant DE with dexamethasone in three of the brain regions, the amygdala, the vDG and the dDG,  
380 but in all brain regions the direction of change was the same (decrease following dexamethasone  
381 treatment; Fig 5A). While *Tcf4* did not show statistically significant DE in the PFC, previous work in this  
382 brain region using co-expression network analysis in human postmortem brain samples [55], has  
383 identified *Tcf4* as a master regulator in schizophrenia. When constructing a DN around *Tcf4* in the PFC,  
384 we identified 26 differentially connected genes including connections to DE genes (n=4) as well as  
385 differential hub genes (n=3, Fig 5B). The *Tcf4* PFC DN was enriched for genes that have been associated  
386 in GWAS with schizophrenia, autism and other neurobehavioral traits (Fig 5C and Table S31). This

387 supports the observation that *Tcf4* networks are relevant for schizophrenia and adds the additional  
388 layer of the importance of *Tcf4* networks in the context of stress. Interestingly, the differential *Tcf4*  
389 network was not only enriched for GO terms related to development, but also autophagy and  
390 chromatin organization (Fig 5D and Table S32).

391 In contrast to the PFC, *Tcf4* was significantly downregulated in the dorsal and ventral dentate gyrus  
392 (Fig 5A). *Tcf4* is highly expressed in the hippocampal formation from the end of prenatal life and  
393 throughout adulthood [53]. We now aimed to use DiffBrainNet to investigate whether *Tcf4* being  
394 differentially expressed in the vDG and dDG of the hippocampal formation would have specific effects  
395 on each sub region's molecular connectivity. From the 55 members of the *Tcf4* vDG and dDG DNs (Fig  
396 5E), 20 are known *Tcf4* targets and/or protein interactors, according to the CHEA and TRANSFAC  
397 transcription factor targets databases [56,57] and the Pathway commons protein-protein interactions  
398 datasets [58]. An additional 11 genes are predicted *Tcf4* targets according to the MotifMap [59] and  
399 TRANSFAC [57] (S4 Fig and Table S33) (datasets assembled by the Harmonizome database, [60]). While  
400 most of the differential connections in this network were regulated in the same direction in both the  
401 vDG and the dDG, we also observed specific differential connections (n=24) that were regulated in an  
402 opposite manner between the two brain regions (Table S34 and selected ones in Fig 5F). *Tcf4*  
403 connections with the group of *Zic* genes, *Zic1*, *Zic2* and *Zic3*, suggested a positive regulatory effect (see  
404 Methods for explanation of term and S1B Fig) in vDG and a negative regulatory effect in dDG. *Zic* genes  
405 have been reported to play an important role in body pattern formation via the Wnt pathway [61], a  
406 pathway that has been extensively associated with *Tcf4* [62,63]. In addition, *Tcf4* had a positive  
407 regulatory connection with *Runx2*, another Wnt pathway effector [64], in dDG and a negative  
408 regulatory connection with it in vDG, suggesting that dexamethasone may mediate *Tcf4* effects on the  
409 Wnt pathway in a DG sub region-specific way. These types of analyses represent a thorough approach  
410 to hypothesis generation for further follow-up experiments of these effects.

411

412



## 413 Discussion

414 The information provided by transcriptomic studies is far richer than a list of differentially expressed  
415 genes. Here, we have derived RNA expression from 8 mouse brain regions at vehicle and treatment  
416 (GCs) conditions and present DiffBrainNet, a resource and analytical framework, that provides access  
417 to DE and DN results. DiffBrainNet allows for direct synthesis and comparisons of the transcriptional  
418 landscape of all 8 brain regions at all conditions (Fig 6A). DiffBrainNet permits the search of DE genes  
419 unique to one brain region or common to any region combination at multiple FDR and fold-change  
420 cutoffs, the generation of plots and the chance to download the data (Fig 6C and 6D). In addition,  
421 DiffBrainNet offers the possibility to visualize the control (vehicle-treated), treatment  
422 (dexamethasone-treated) and differential networks in a single brain region and in any region  
423 combination, the ability to compare hub genes on all treatment levels at multiple node-betweenness  
424 thresholds and to download the network plots and data (Fig 6B and 6D).

425 Comparing networks between two conditions is associated with a number of issues, as highlighted by  
426 De la Fuente [4] and described below. Comparison of networks uses mainly the node degree, which is  
427 a measure of a gene's number of connections in two networks. This approach is highly dependent on  
428 the threshold that is used for the edges that are included in the two different networks and has proven  
429 challenging, since it is unclear how to choose comparable thresholds for two different networks. We  
430 sought to overcome this challenge by computing a single DN. We established a two-step method in  
431 order to differentially analyze networks. First, we used KiMONo to compute prior knowledge-based  
432 networks at vehicle-treated and following dexamethasone administration (treatment) conditions.  
433 Second, DNs were computed using DiffGRN. DiffGRN uses a z-test to calculate differential gene  
434 interactions based on the regression  $\beta$ -values of gene pairs at the vehicle and treatment network (S1B  
435 Fig) [25]. This approach provides differential interactions, thus eliminating the problem of having to  
436 compare two networks. This way we could pinpoint not only which genes but also which interactions  
437 of specific genes mediate the network changes. Moreover, by using prior-knowledge guided networks  
438 (KiMONo) [3], in which the expression of each gene is modeled by using the genes/proteins connected

439 to it in a prior network as possible predictors in the regression model, we could compute vehicle and  
440 treatment networks of the same topological layout. This allowed for an even more robust comparison  
441 and reliable calculation of the z-values for the DN.

442 The use of biological knowledge in the form of a prior network, upon which the vehicle and treatment  
443 networks are built, is a substantial difference of KiMONo as compared to other network approaches  
444 such as weighted correlation network analysis (WGCNA) [2], which are built using correlation matrices  
445 without the use of prior- biological knowledge. DiffBrainNet is limited by a restricted search space,  
446 since it can only model interactions present in the prior network we chose to use. In the present  
447 analysis and the DiffBrainNet resource, we used FunCoup 5 to build our prior network [37]. FunCoup  
448 infers functional associations of genes or proteins using various data types and sources, including  
449 transcription factor binding sites, cellular and subcellular colocalization and protein-protein  
450 interactions. The use of such functional associations on the gene or protein level inferred by a variety  
451 of experimental data as prior-knowledge for predicting networks reduces the risk of false positives  
452 since the search space is restricted to known interactions and adds functional protein-level  
453 information to the transcriptomic data. Since, we provide the source code of all analysis  
454 (<https://github.molgen.mpg.de/mpip/DiffBrainNet>), a suitable prior network according to each  
455 research question can be chosen thus providing flexibility and specificity in hypothesis testing. By using  
456 prior-knowledge, the network metrics (node-degree, node-betweenness, modularity) are influenced  
457 by the prior network. To overcome this, we used normalized node-betweenness for all our analyses,  
458 which is defined as the node-betweenness in the calculated network divided by the prior network  
459 node-betweenness.

460 The combination of both gene- and network level analysis enriches our understanding of  
461 transcriptomic data and of biological implications. We showed that differential prior knowledge-based  
462 network analysis can unravel different and complementary aspects of the transcriptomic responses to  
463 a treatment as compared to individual gene-level analysis (DE). For example, we showed that in the  
464 PFC neither of the differential hub genes were also DE genes and that DE and DN analyses revealed

465 distinct aspects of the transcriptomic responses. The DE genes explained effects mainly on signaling  
466 and development whereas the members of the DN explained mainly the cellular responses to the  
467 stimulus, GCs which are the main stress hormones, and stress.

468 DNs can be used to resolve underlying biological responses that are not detected by DE analysis. We  
469 identified *Abcd1* as the top differential hub gene in the PFC, which was not detected as a DE gene  
470 itself. ABC proteins are actively transporting GCs, including dexamethasone across the blood brain  
471 barrier and the placenta [50,51]. ABC transporters, synaptic biology and neuropsychiatric phenotypes  
472 have been previously associated in the literature. *Abcd1*- deficient microglia have been correlated with  
473 synaptic loss and axonopathy [65] pointing to an *Abcd1*-dysregulated network association with  
474 synaptic signaling problems. *Abcb1*, another member of the ABC transporters family, has been  
475 associated with stress adaptation and potential mediation of stress-related psychiatric disorders  
476 phenotypes [66]. These findings highlighted that the exclusive analysis of transcriptomic data at the  
477 gene-level does not capture all aspects of the transcriptional response to a stimulus, and the DN  
478 analysis can unravel distinct but complementary aspects that can lead to specific molecular pathways  
479 identification.

480 Finally, networks can be used for hypothesis generation and testing by choosing a suitable prior  
481 network. This approach can be exploited to generate hypotheses regarding the interactive effects of  
482 environmental exposures and the molecular underpinnings of specific genes. Using DiffBrainNet we  
483 analyzed the effects of dexamethasone on the co-expression network of a major psychiatric risk gene,  
484 *Tcf4*, in 3 different brain regions. *Tcf4* is expressed in the cortex, the hippocampus and the  
485 hypothalamic and amygdaloid nuclei predominantly at the end of prenatal life decreasing to lower  
486 expression levels throughout adulthood [53] and was shown to regulate neural progenitor cell  
487 maintenance and proliferation [67]. Animal models of gain and loss of function of *Tcf4* have shown its  
488 relevance for cognition, sensorimotor gating and neuroplasticity [68]. In addition, gene x psychosocial  
489 stress interactions have been reported for *Tcf4* [69], but little is known about relevant molecular  
490 pathways and brain regions for this interaction. With DiffBrainNet we showed that *Tcf4* mediates GCs

491 effects in two sub-regions of the hippocampal formation, ventral and dorsal DG, at the gene- and at  
492 the network- levels since it is DE in those but only at the network-level for the PFC where is not a DE  
493 gene. The PFC DN of *Tcf4* was enriched for terms that include autophagy. The connection of *Tcf4* and  
494 autophagy has been previously described in the literature [62] but this is to our knowledge, the first  
495 report of a potential role of *Tcf4* in stress-related regulation of autophagy. This approach can be  
496 extended to the investigation of a wide spectrum of different gene lists - produced by GWAS studies  
497 for example - both at vehicle and after glucocorticoid exposure in a brain region-specific manner using  
498 DiffBrainNet. The results can be used to design more focused experiments to resolve targeted  
499 molecular mechanisms implicated in the pathogenesis of brain disorders.

500 In summary, through DN analysis we were able to identify specific molecular connectivity patterns  
501 governing transcriptomic responses to glucocorticoids that are not unraveled when investigating the  
502 differential gene expression levels alone. In our dataset, we inferred DNs in 8 mouse brain regions  
503 including a detailed segmentation of the hippocampal formation. With this work, we introduce  
504 DiffBrainNet, a resource and an analytical framework that includes both gene expression data and  
505 prior-guided genome-wide networks in these 8 brain regions at control (vehicle-treated), following  
506 GCs stimulation and at the differential level. DiffBrainNet can be used to pinpoint molecular pathways  
507 important for the basic function and response to GCs in a brain-region specific manner. It can also  
508 support the identification and analysis of biological processes regulated by brain and psychiatric  
509 diseases risk genes at the control and differential levels. We made these complex datasets and  
510 analyses available to all interested researchers via DiffBrainNet (access:  
511 <http://diffbrainnet.psych.mpg.de>, Fig 6).

512

### 513 **Data availability**

514 Raw and normalized gene expression data generated in this study are provided at GEO under  
515 GSE190712 (<https://www.ncbi.nlm.nih.gov/geo/query/acc.cgi?acc=GSE190712>). Differential  
516 expression and differential network data can be downloaded from our resource DiffBrainNet.

517 **Code availability**

518 Data analysis scripts and scripts that were used to generate the manuscript figures is available via  
519 github: <https://github.molgen.mpg.de/mpip/DiffBrainNet>. The source code of the shiny app is  
520 available via github as well: [https://github.molgen.mpg.de/mpip/DiffBrainNet\\_ShinyApp](https://github.molgen.mpg.de/mpip/DiffBrainNet_ShinyApp).

521

522 **Author contributions**

523 ACK and NG are joint first authors, contributed equally to this work and are listed alphabetically. ACK  
524 designed and carried out experiments, performed enrichment analyses, provided critical intellectual  
525 input and generated the paper draft; NG performed the differential expression and network analysis,  
526 implemented the resource as R shiny app, provided critical intellectual input and generated the paper  
527 draft; CC designed experiments, provided critical intellectual input and revised the paper draft; SR pre-  
528 processed the sequencing data; BP deployed and hosted the shiny app; MVS designed and carried out  
529 experiments and provided critical intellectual input; SS performed libraries preparation; MRH  
530 supported project organization and experimental procedures; JKA and EBB contributed equally to this  
531 work and are joint corresponding authors. JKA and EBB conceived the idea, obtained funding,  
532 supervised the study, designed experiments and analysis pipelines, provided critical intellectual input  
533 and contributed to paper draft writing.

534

535 **Acknowledgments**

536 We thank the Biomaterial processing and repository unit (BioPrep) of the Max Planck Institute of  
537 Psychiatry for their contribution on RNA isolation. We thank Jonas Hagenberg for his help on the  
538 implementation of the Shiny app. NG is supported by the Joachim Herz Foundation.

539

540 **Citations**

541 1. Subramanian A, Tamayo P, Mootha VK, Mukherjee S, Ebert BL, Gillette MA, et al. Gene set  
542 enrichment analysis: A knowledge-based approach for interpreting genome-wide expression

- 543 profiles. Proceedings of the National Academy of Sciences of the United States of America.  
544 2005;102: 15545–15550. doi:10.1073/pnas.0506580102
- 545 2. Langfelder P, Horvath S. WGCNA: An R package for weighted correlation network analysis.  
546 BMC Bioinformatics. 2008;9. doi:10.1186/1471-2105-9-559
- 547 3. Ogris C, Hu Y, Arloth J, Müller NS. Versatile knowledge guided network inference method for  
548 prioritizing key regulatory factors in multi-omics data. Scientific Reports. 2021;11: 1–12.  
549 doi:10.1038/s41598-021-85544-4
- 550 4. de la Fuente A. From “differential expression” to “differential networking” - identification of  
551 dysfunctional regulatory networks in diseases. Trends in Genetics. 2010;26: 326–333.  
552 doi:10.1016/j.tig.2010.05.001
- 553 5. Parikshak NN, Gandal MJ, Geschwind DH. Systems biology and gene networks in  
554 neurodevelopmental and neurodegenerative disorders. Nature Reviews Genetics. 2015;16:  
555 441–458. doi:10.1038/nrg3934
- 556 6. Li X, Zhang Y, Wang L, Lin Y, Gao Z, Zhan X, et al. Integrated Analysis of Brain Transcriptome  
557 Reveals Convergent Molecular Pathways in Autism Spectrum Disorder. Frontiers in  
558 Psychiatry. 2019;10: 1–8. doi:10.3389/fpsyt.2019.00706
- 559 7. Kapoor M, Wang JC, Farris SP, Liu Y, McClintick J, Gupta I, et al. Analysis of whole genome-  
560 transcriptomic organization in brain to identify genes associated with alcoholism.  
561 Translational Psychiatry. 2019;9. doi:10.1038/s41398-019-0384-y
- 562 8. Sato K, Mano T, Matsuda H, Senda M, Ihara R, Suzuki K, et al. Visualizing modules of  
563 coordinated structural brain atrophy during the course of conversion to Alzheimer’s disease  
564 by applying methodology from gene co-expression analysis. NeuroImage: Clinical. 2019;24:  
565 101957. doi:10.1016/j.nicl.2019.101957
- 566 9. Bowen EFW, Burgess JL, Granger R, Kleinman JE, Rhodes CH. DLPFC transcriptome defines  
567 two molecular subtypes of schizophrenia. Translational Psychiatry. 2019;9: 1–10.  
568 doi:10.1038/s41398-019-0472-z

- 569 10. Kwon J, Kim YJ, Choi K, Seol S, Kang HJ. Identification of stress resilience module by weighted  
570 gene co-expression network analysis in Fkbp5-deficient mice. *Molecular Brain*. 2019;12: 10–  
571 13. doi:10.1186/s13041-019-0521-9
- 572 11. Zimmermann CA, Arloth J, Santarelli S, Löschner A, Weber P, Schmidt M V., et al. Stress  
573 dynamically regulates co-expression networks of glucocorticoid receptor-dependent MDD  
574 and SCZ risk genes. *Translational Psychiatry*. 2019;9: 1–11. doi:10.1038/s41398-019-0373-1
- 575 12. Labonté B, Engmann O, Purushothaman I, Menard C, Wang J, Tan C, et al. Sex-specific  
576 transcriptional signatures in human depression. *Nature Medicine*. 2017;23: 1102–1111.  
577 doi:10.1038/nm.4386
- 578 13. Geng R, Li Z, Yu S, Yuan C, Hong W, Wang Z, et al. Weighted gene co-expression network  
579 analysis identifies specific modules and hub genes related to subsyndromal symptomatic  
580 depression. *World Journal of Biological Psychiatry*. 2020;21: 102–110.  
581 doi:10.1080/15622975.2018.1548782
- 582 14. Bagot RCC, Cates HMM, Purushothaman I, Lorsch ZSS, Walker DMM, Wang J, et al. Circuit-  
583 wide Transcriptional Profiling Reveals Brain Region-Specific Gene Networks Regulating  
584 Depression Susceptibility. *Neuron*. 2016;90: 969–983. doi:10.1016/j.neuron.2016.04.015
- 585 15. Huggett SB, Stallings MC. Cocaine’omics: Genome-wide and transcriptome-wide analyses  
586 provide biological insight into cocaine use and dependence. *Addiction Biology*. 2020;25: 1–10.  
587 doi:10.1111/adb.12719
- 588 16. Liu J, Jing L, Tu X. Weighted gene co-expression network analysis identifies specific modules  
589 and hub genes related to coronary artery disease. *BMC Cardiovascular Disorders*. 2016;16: 1–  
590 8. doi:10.1186/s12872-016-0217-3
- 591 17. Pierson E, Koller D, Battle A, Mostafavi S. Sharing and Specificity of Co-expression Networks  
592 across 35 Human Tissues. *PLoS Computational Biology*. 2015;11: 1–19.  
593 doi:10.1371/journal.pcbi.1004220
- 594 18. Sondka Z, Bamford S, Cole CG, Ward SA, Dunham I, Forbes SA. The COSMIC Cancer Gene

- 595 Census: describing genetic dysfunction across all human cancers. *Nature Reviews Cancer*.  
596 2018;18: 696–705. doi:10.1038/s41568-018-0060-1
- 597 19. Perduca V, Omichessan H, Baglietto L, Severi G. Mutational and epigenetic signatures in  
598 cancer tissue linked to environmental exposures and lifestyle. *Current Opinion in Oncology*.  
599 2018;30: 61–67. doi:10.1097/CCO.0000000000000418
- 600 20. Akbarian S, Liu C, Knowles JA, Vaccarino FM, Farnham PJ, Crawford GE, et al. The  
601 PsychENCODE project. *Nature Neuroscience*. 2015;18: 1707–1712. doi:10.1038/nn.4156
- 602 21. Li M, Santpere G, Kawasawa YI, Evgrafov O V., Gulden FO, Pochareddy S, et al. Integrative  
603 functional genomic analysis of human brain development and neuropsychiatric risks. *Science*.  
604 2018;362. doi:10.1126/science.aat7615
- 605 22. Gandal MJ, Haney JR, Parikshak NN, Leppa V, Ramaswami G, Hartl C, et al. Shared molecular  
606 neuropathology across major psychiatric disorders parallels polygenic overlap. *Science*.  
607 2018;359: 693–697. doi:10.1126/science.aad6469
- 608 23. Saint-Antoine MM, Singh A. Network inference in systems biology: recent developments,  
609 challenges, and applications. *Current Opinion in Biotechnology*. Elsevier Ltd; 2020. pp. 89–98.  
610 doi:10.1016/j.copbio.2019.12.002
- 611 24. Linde J, Schulze S, Henkel SG, Guthke R. Data- and knowledge-based modeling of gene  
612 regulatory networks: an update. *EXCLI journal*. 2015;14: 346–378. doi:10.17179/excli2015-  
613 168
- 614 25. Kim Youngsoon, Jie Hao, Yadu Gautam, Tesfaye B. Mersha MK. DiffGRN: differential gene  
615 regulatory network analysis. *International Journal of Data Mining and Bioinformatics*.  
616 2018;20: 362. doi:10.1504/ijdmb.2018.10016325
- 617 26. Weikum ER, Knuesel MT, Ortlund EA, Yamamoto KR. Glucocorticoid receptor control of  
618 transcription : precision and plasticity via allostery. doi:10.1038/nrm.2016.152
- 619 27. Mcewen BS, Akil H. Revisiting the Stress Concept : Implications for Affective Disorders.  
620 2020;40: 12–21.



- 621 28. George Paxinos and Keith B. J. Franklin. The mouse brain in stereotaxic coordinates.  
622 Academic Press; 2001. doi:10.1016/s0306-4530(03)00088-x
- 623 29. Andrews Simon, Krueger Felix, Segonds-Pichon Anne, Biggins Laura, Krueger Christel MJ.  
624 fastQC. 2019. Available: <https://www.bioinformatics.babraham.ac.uk/projects/fastqc/>
- 625 30. Martin M. Cutadapt removes adapter sequences from high-throughput sequencing reads.  
626 Available: <https://doi.org/10.14806/ej.17.1.200>
- 627 31. Smith T, Heger A, Sudbery I. UMI-tools: Modeling sequencing errors in Unique Molecular  
628 Identifiers to improve quantification accuracy. *Genome Research*. 2017;27: 491–499.  
629 doi:10.1101/gr.209601.116
- 630 32. Dobin A, Davis CA, Schlesinger F, Drenkow J, Zaleski C, Jha S, et al. STAR: Ultrafast universal  
631 RNA-seq aligner. *Bioinformatics*. 2013;29: 15–21. doi:10.1093/bioinformatics/bts635
- 632 33. Liao Y, Smyth GK, Shi W. FeatureCounts: An efficient general purpose program for assigning  
633 sequence reads to genomic features. *Bioinformatics*. 2014;30: 923–930.  
634 doi:10.1093/bioinformatics/btt656
- 635 34. R: A language and environment for statistical computing. R Foundation for Statistical  
636 Computing, Vienna, Austria. 2021. Available: <https://www.r-project.org/>
- 637 35. Leek JT, Johnson WE, Parker HS, Jaffe AE, Storey JD. The SVA package for removing batch  
638 effects and other unwanted variation in high-throughput experiments. *Bioinformatics*.  
639 2012;28: 882–883. doi:10.1093/bioinformatics/bts034
- 640 36. Love MI, Huber W, Anders S. Moderated estimation of fold change and dispersion for RNA-  
641 seq data with DESeq2. *Genome Biology*. 2014;15. doi:10.1186/s13059-014-0550-8
- 642 37. Persson E, Castresana-Aguirre M, Buzzao D, Guala D, Sonhammer ELL. FunCoup 5:  
643 Functional Association Networks in All Domains of Life, Supporting Directed Links and Tissue-  
644 Specificity. *Journal of Molecular Biology*. 2021;433: 166835. doi:10.1016/j.jmb.2021.166835
- 645 38. Csardi G. The Igraph Software Package for Complex Network Research. 2014. Available:  
646 <https://www.researchgate.net/publication/221995787>

- 647 39. Watanabe K, Taskesen E, Van Bochoven A, Posthuma D. Functional mapping and annotation  
648 of genetic associations with FUMA. *Nature Communications*. 2017;8. doi:10.1038/s41467-  
649 017-01261-5
- 650 40. Carbon S, Douglass E, Good BM, Unni DR, Harris NL, Mungall CJ, et al. The Gene Ontology  
651 resource: Enriching a GOld mine. *Nucleic Acids Research*. 2021;49: D325–D334.  
652 doi:10.1093/nar/gkaa1113
- 653 41. Ashburner M, Ball CA, Blake JA, Botstein D, Butler H, Cherry JM, et al. Gene ontology: Tool for  
654 the unification of biology. *Nature Genetics*. 2000;25: 25–29. doi:10.1038/75556
- 655 42. Kanehisa M, Furumichi M, Sato Y, Ishiguro-Watanabe M, Tanabe M. KEGG: Integrating viruses  
656 and cellular organisms. *Nucleic Acids Research*. 2021;49: D545–D551.  
657 doi:10.1093/nar/gkaa970
- 658 43. Kanehisa M, Goto S. KEGG: Kyoto Encyclopedia of Genes and Genomes. *Nucleic Acids*  
659 *Research*. 2000;28: 27–30. doi:10.1093/nar/28.1.27
- 660 44. Kanehisa M. Toward understanding the origin and evolution of cellular organisms. *Protein*  
661 *Science*. 2019;28: 1947–1951. doi:10.1002/pro.3715
- 662 45. Jassal B, Matthews L, Viteri G, Gong C, Lorente P, Fabregat A, et al. The reactome pathway  
663 knowledgebase. *Nucleic Acids Research*. 2020;48: D498–D503. doi:10.1093/nar/gkz1031
- 664 46. Buniello A, Macarthur JAL, Cerezo M, Harris LW, Hayhurst J, Malangone C, et al. The NHGRI-  
665 EBI GWAS Catalog of published genome-wide association studies, targeted arrays and  
666 summary statistics 2019. *Nucleic Acids Research*. 2019;47: D1005–D1012.  
667 doi:10.1093/nar/gky1120
- 668 47. Benjamini Y, Hochberg Y. Controlling the False Discovery Rate: A Practical and Powerful  
669 Approach to Multiple Testing. Source: *Journal of the Royal Statistical Society Series B*  
670 (Methodological). 1995.
- 671 48. Shiny From RStudio. Available: <https://shiny.rstudio.com/>
- 672 49. Open Analytics. ShinyProxy. Available: <https://www.shinyproxy.io/>

- 673 50. Uhr M, Holsboer F, Müller MB. Penetration of endogenous steroid hormones corticosterone,  
674 cortisol, aldosterone and progesterone into the brain is enhanced in mice deficient for both  
675 mdr1a and mdr1b P-glycoproteins. *Journal of Neuroendocrinology*. 2002;14: 753–759.  
676 doi:10.1046/j.1365-2826.2002.00836.x
- 677 51. Müller MB, Keck ME, Binder EB, Kresse AE, Hagemeyer TP, Landgraf R, et al. ABCBI (MDRI)-  
678 Type P-Glycoproteins at the Blood-Brain Barrier Modulate the Activity of the Hypothalamic-  
679 Pituitary-Adrenocortical System: Implications for Affective Disorder.  
680 *Neuropsychopharmacology*. 2003;28: 1991–1999. doi:10.1038/sj.npp.1300257
- 681 52. Luo X, Rosenfeld JA, Yamamoto S, Harel T, Zuo Z, Hall M, et al. Clinically severe CACNA1A  
682 alleles affect synaptic function and neurodegeneration differentially. *PLoS Genetics*. 2017;13.  
683 doi:10.1371/journal.pgen.1006905
- 684 53. Teixeira JR, Szeto RA, Carvalho VMA, Muotri AR, Papes F. Transcription factor 4 and its  
685 association with psychiatric disorders. *Translational Psychiatry*. 2021;11. doi:10.1038/s41398-  
686 020-01138-0
- 687 54. Sirp A, Roots K, Nurm K, Tuvikene J, Sepp M, Timmusk T. Functional consequences of TCF4  
688 missense substitutions associated with Pitt-Hopkins syndrome , mild intellectual disability ,  
689 and schizophrenia. 2021;1: 1–16. doi:10.1016/j.jbc.2021.101381
- 690 55. Torshizi AD, Armoskus C, Zhang H, Forrest MP, Zhang S, Souaiaia T, et al. Deconvolution of  
691 transcriptional networks identifies TCF4 as a master regulator in schizophrenia. *Science*  
692 *Advances*. 2019;5. doi:10.1126/sciadv.aau4139
- 693 56. Lachmann A, Xu H, Krishnan J, Berger SI, Mazloom AR, Ma'ayan A. ChEA: transcription factor  
694 regulation inferred from integrating genome-wide ChIP-X experiments. *Bioinformatics*  
695 (Oxford, England). 2010/08/13. 2010;26: 2438–2444. doi:10.1093/bioinformatics/btq466
- 696 57. Wingender E, Dietze P, Karas H, Knüppel R. TRANSFAC: A Database on Transcription Factors  
697 and Their DNA Binding Sites. *Nucleic Acids Research*. 1996;24: 238–241.  
698 doi:10.1093/nar/24.1.238

- 699 58. Cerami EG, Gross BE, Demir E, Rodchenkov I, Babur Ö, Anwar N, et al. Pathway Commons, a  
700 web resource for biological pathway data. *Nucleic Acids Research*. 2011;39: D685–D690.  
701 doi:10.1093/nar/gkq1039
- 702 59. Liu Y, Sun S, Bredy T, Wood M, Spitale RC, Baldi P. MotifMap-RNA: a genome-wide map of  
703 RBP binding sites. *Bioinformatics*. 2017;33: 2029–2031. doi:10.1093/bioinformatics/btx087
- 704 60. Rouillard AD, Gundersen GW, Fernandez NF, Wang Z, Monteiro CD, McDermott MG, et al.  
705 The harmonizome: a collection of processed datasets gathered to serve and mine knowledge  
706 about genes and proteins. *Database : the journal of biological databases and curation*.  
707 2016;2016: 1–16. doi:10.1093/database/baw100
- 708 61. Nagai T, Aruga J, Takada S, Günther T, Spörle R, Schughart K, et al. The expression of the  
709 mouse *Zic1*, *Zic2*, and *Zic3* gene suggests an essential role for *Zic* genes in body pattern  
710 formation. *Developmental Biology*. 1997;182: 299–313. doi:10.1006/dbio.1996.8449
- 711 62. Petherick KJ, Williams AC, Lane JD, Ordóñez-Morán P, Huelsken J, Collard TJ, et al.  
712 Autolysosomal  $\beta$ -catenin degradation regulates Wnt-autophagy-p62 crosstalk. *EMBO Journal*.  
713 2013;32: 1903–1916. doi:10.1038/emboj.2013.123
- 714 63. Bem J, Brożko N, Chakraborty C, Lipiec MA, Koziński K, Nagalski A, et al. Wnt/ $\beta$ -catenin  
715 signaling in brain development and mental disorders: keeping TCF7L2 in mind. *FEBS Letters*.  
716 2019;593: 1654–1674. doi:10.1002/1873-3468.13502
- 717 64. McCarthy TL, Centrella M. Novel links among Wnt and TGF- $\beta$  signaling and Runx2. *Molecular*  
718 *Endocrinology*. 2010;24: 587–597. doi:10.1210/me.2009-0379
- 719 65. Gong Y, Sasidharan N, Laheji F, Frosch M, Musolino P, Tanzi R, et al. Microglial dysfunction as  
720 a key pathological change in adrenomyeloneuropathy. *Annals of Neurology*. 2017;82: 813–  
721 827. doi:10.1002/ana.25085
- 722 66. Lopez JP, Brivio E, Santambrogio A, De Donno C, Kos A, Peters M, et al. Single-cell molecular  
723 profiling of all three components of the HPA axis reveals adrenal ABCB1 as a regulator of  
724 stress adaptation. *Science Advances*. 2021;7: 1–18. doi:10.1126/sciadv.abe4497

- 725 67. Mesman S, Bakker R, Smidt MP. Tcf4 is required for correct brain development during  
726 embryogenesis. *Molecular and Cellular Neuroscience*. 2020;106: 103502.  
727 doi:10.1016/j.mcn.2020.103502
- 728 68. Badowska DM, Brzózka MM, Kannaiyan N, Thomas C, Dibaj P, Chowdhury A, et al. Modulation  
729 of cognition and neuronal plasticity in gain- and loss-of-function mouse models of the  
730 schizophrenia risk gene Tcf4. *Translational Psychiatry*. 2020;10. doi:10.1038/s41398-020-  
731 01026-7
- 732 69. Volkman P, Stephan M, Krackow S, Jensen N, Rossner MJ. PsyCoP – A Platform for  
733 Systematic Semi-Automated Behavioral and Cognitive Profiling Reveals Gene and  
734 Environment Dependent Impairments of Tcf4 Transgenic Mice Subjected to Social Defeat.  
735 *Frontiers in Behavioral Neuroscience*. 2021;14: 1–15. doi:10.3389/fnbeh.2020.618180  
736  
737

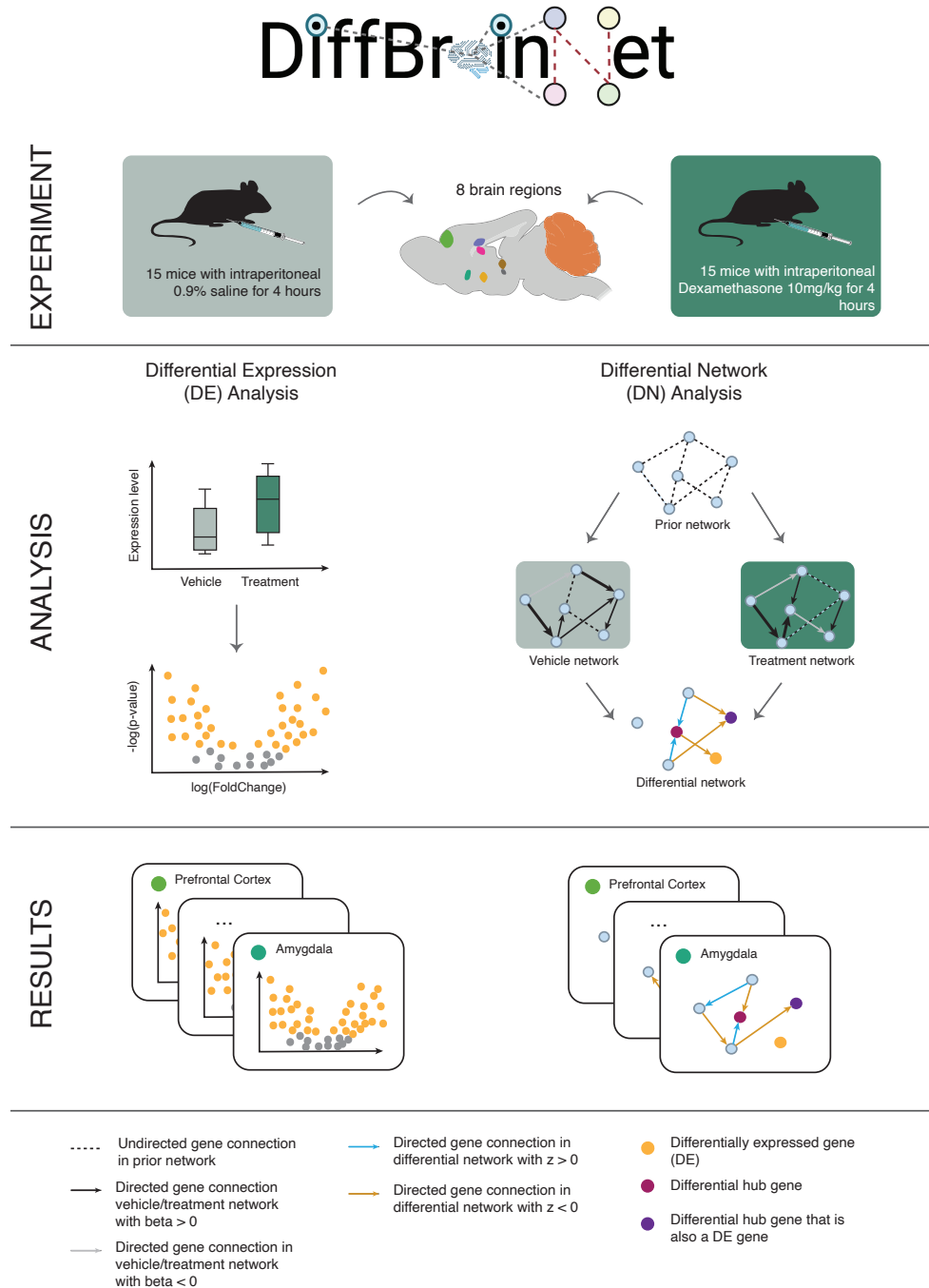


**Figure 1: Schematic representation of experimental and analytical steps.** DiffBrainNet is a resource of differential expression and differential networks in 8 mouse brain regions. (Experiment) *C57Bl/6* mice were treated intraperitoneally with 10mg/kg Dexamethasone or 0.9% saline as vehicle for 4hours. Eight different brain regions were isolated: amygdala – AMY, cerebellar cortex – CER, prefrontal cortex – PFC, paraventricular nucleus of the hypothalamus – PVN, dorsal *Cornu Ammonis* 1 – dCA1, ventral *Cornu Ammonis* 1 – vCA1, dorsal dentate gyrus – dDG, ventral dentate gyrus – vDG. (Analysis) We performed RNA sequencing in the 8 brain regions, followed by differential expression analysis (DE) and differential prior-knowledge-based genome-wide network analysis (DN). (Results) DiffBrainNet includes differential expression results and network results for all brain regions. DiffBrainNet logo was created with BioRender.com.

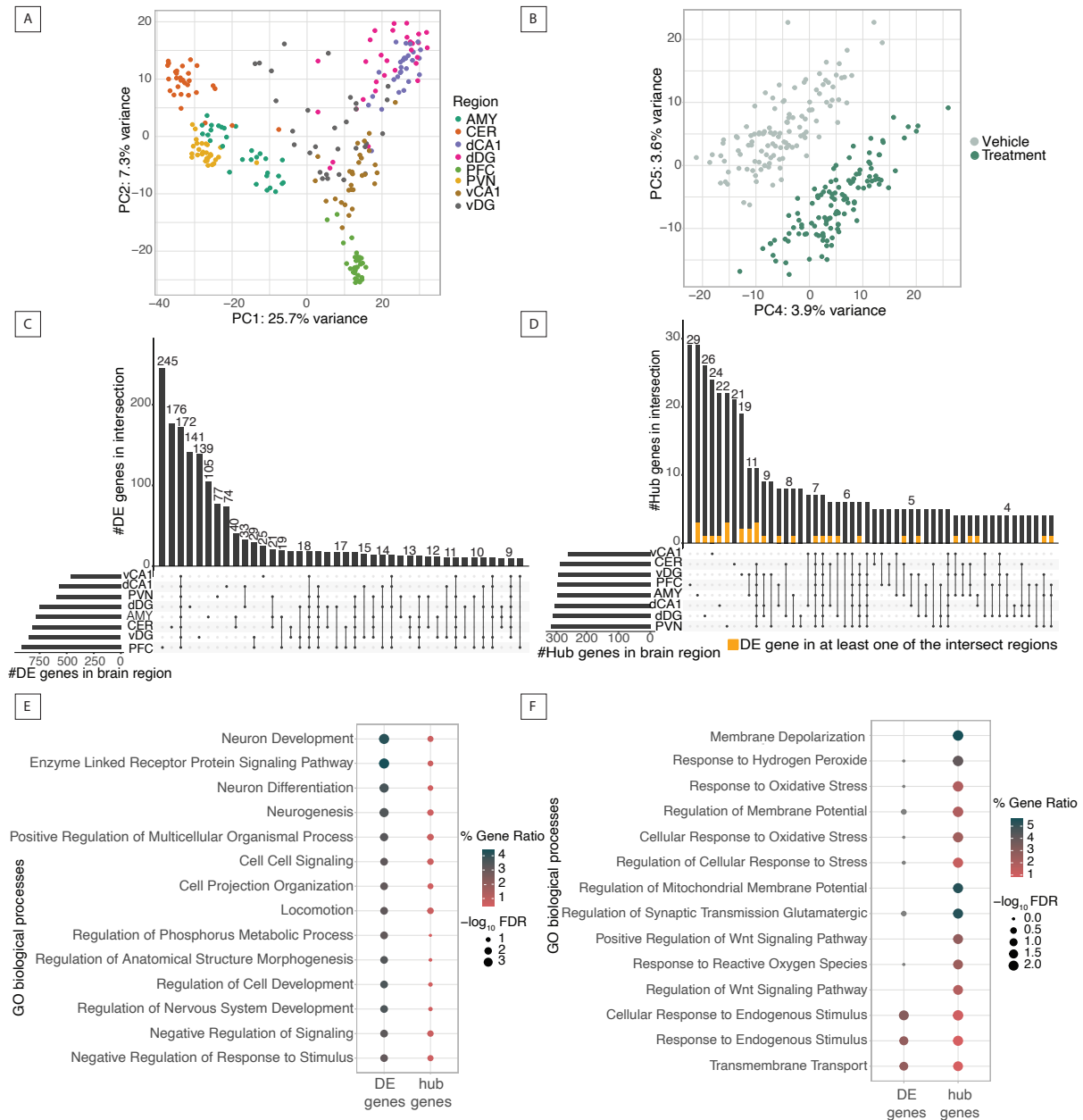


**Figure 2: Differential network analysis provides distinct biological information from differential expression: the case of PFC.** (A) Principal component (PC) analysis plot of PCs 1 and 2 explaining variance associated with brain region. (B) PC analysis plot of PCs 4 and 5 explaining variance associated with treatment group. (C) Upset plot comparing differentially expressed genes with FDR adjusted p-value smaller than 0.1 across 8 brain regions. (D) Upset plot comparing differential hub genes with a normalized node-betweenness above 1.0 across 8 brain regions. Proportions of intersection size bars coloured in yellow indicate genes that are also significantly DE genes in at least one of the intersection's brain regions. (E) Dot plot for the top 14 GO terms most highly enriched for the unique DE genes and (F) for the unique differential hub genes in the PFC. (GO terms enrichment analyses are done with at least 10% of the input genes having to overlap with the genes of the term.)

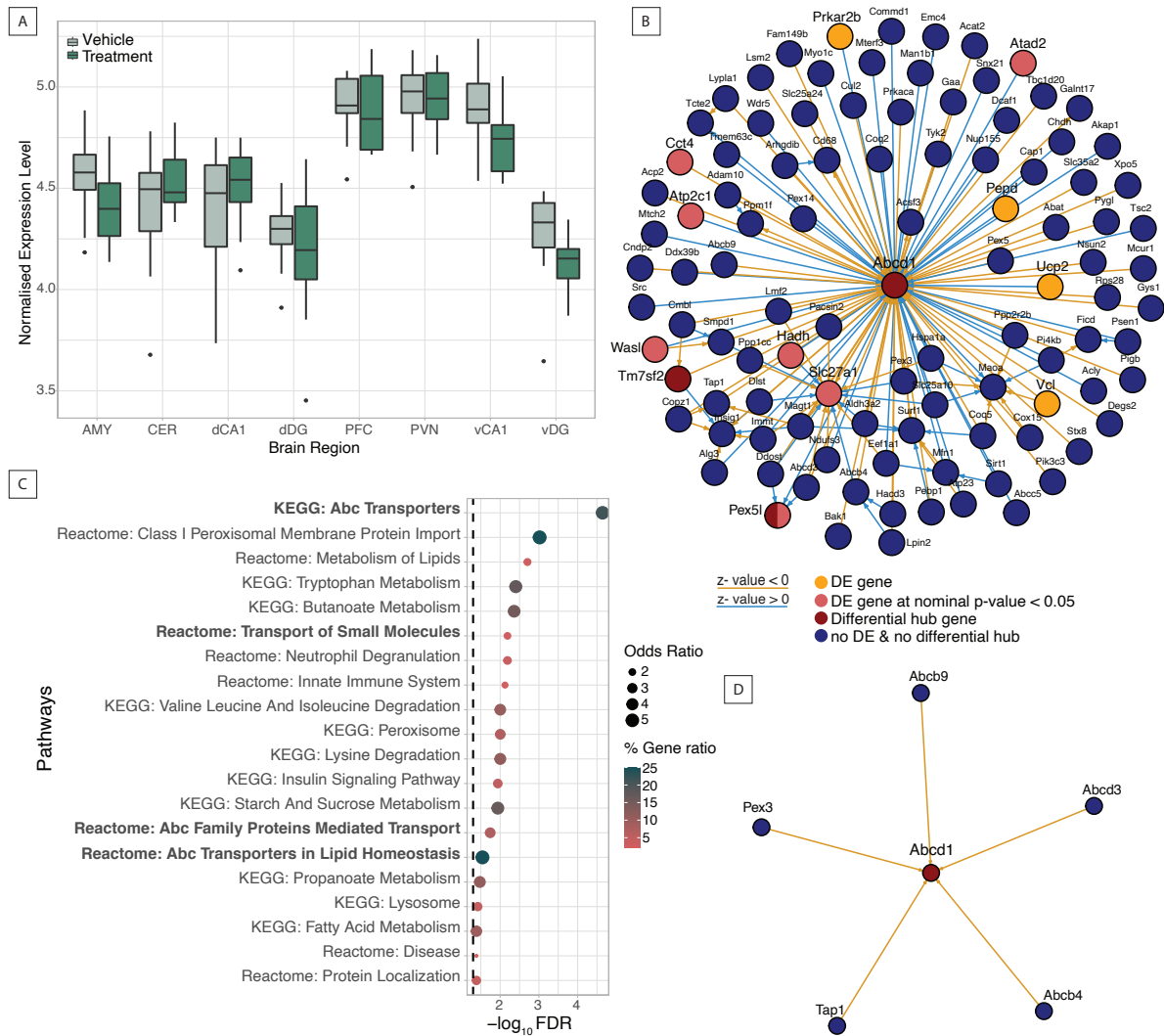


**Figure 3: ABC transporters mediate dexamethasone response in the PFC at the network level.**

(A) Normalized expression of *Abcd1* in all brain regions at vehicle and after dexamethasone administration. *Abcd1* is not differentially expressed in any of the 8 regions. (B) *Abcd1* gene neighborhood in the differential network of the PFC. (C) KEGG and Reactome pathway enrichments for *Abcd1* and its differential neighbors in PFC. Bold labeled terms highlight a more general involvement of the ABC transporters pathway in the PFC response to glucocorticoids. (D) Network representation of the ABC transporters differential pathway.



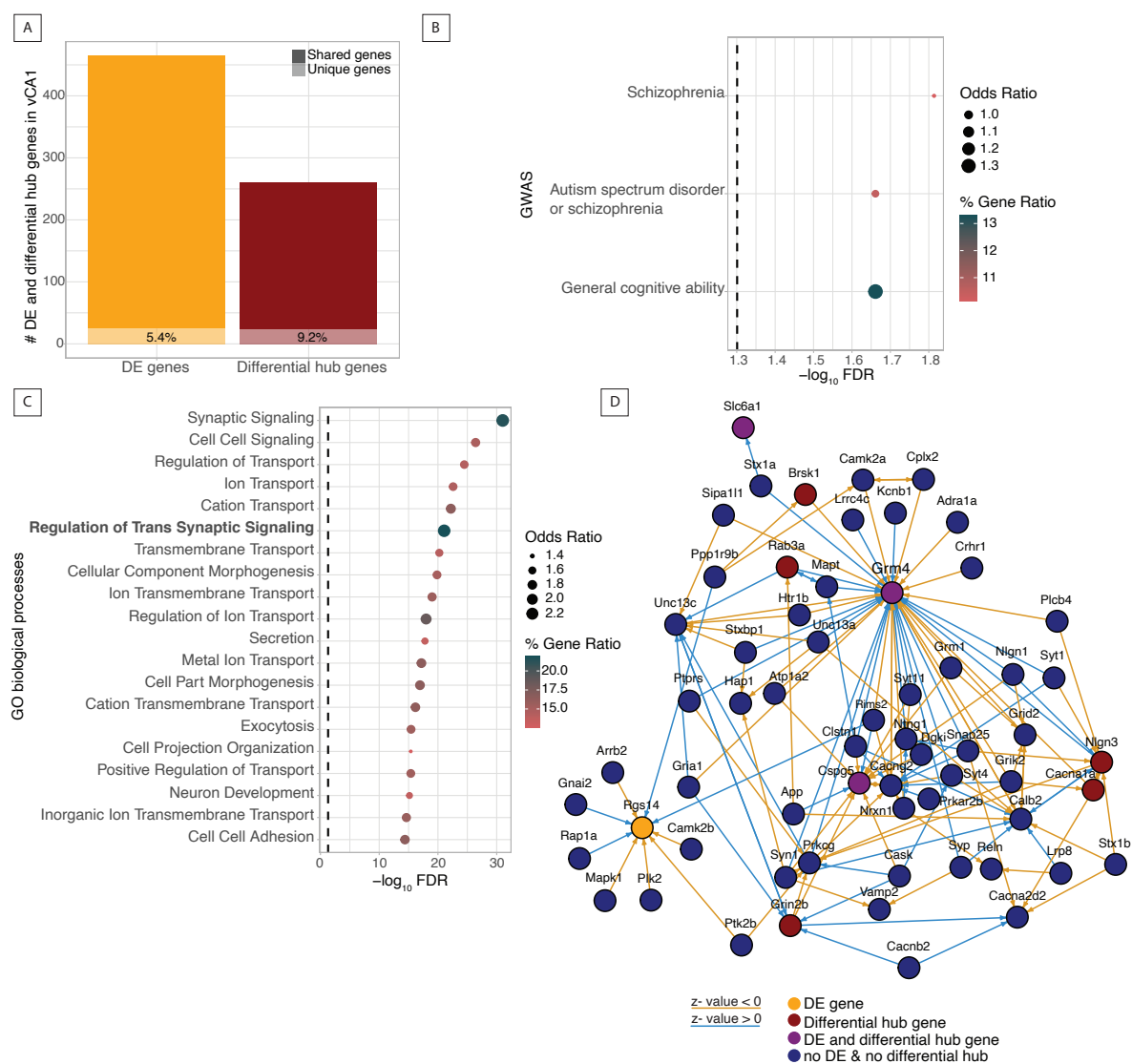


**Figure 4: Differential network analysis supports the biological understanding of differential expression: the case of vCA1.** (A) Number of unique and shared DE genes in vCA1 and number of unique and shared differential hub genes in vCA1. vCA1 has the least unique DE genes but the third highest percentage of unique differential hub genes of the eight brain regions. (B) Unique vCA1 DE genes and their differential neighbors are enriched for genes that carry SNPs associated with the GWAS traits schizophrenia, autism spectrum disorder or schizophrenia and general cognitive ability. (C) GO biological processes enrichment analysis of unique vCA1 DE genes and their neighbors. (D) Differential neighborhood of the genes that are part of the GO term regulation of trans-synaptic signaling and connected with the vCA1 unique DE genes. (GO terms enrichment analysis is done with at least 10% of the input genes having to overlap with the genes of the term. GWAS enrichment analysis is done with 16 of the input genes having to overlap with the genes of the term.)

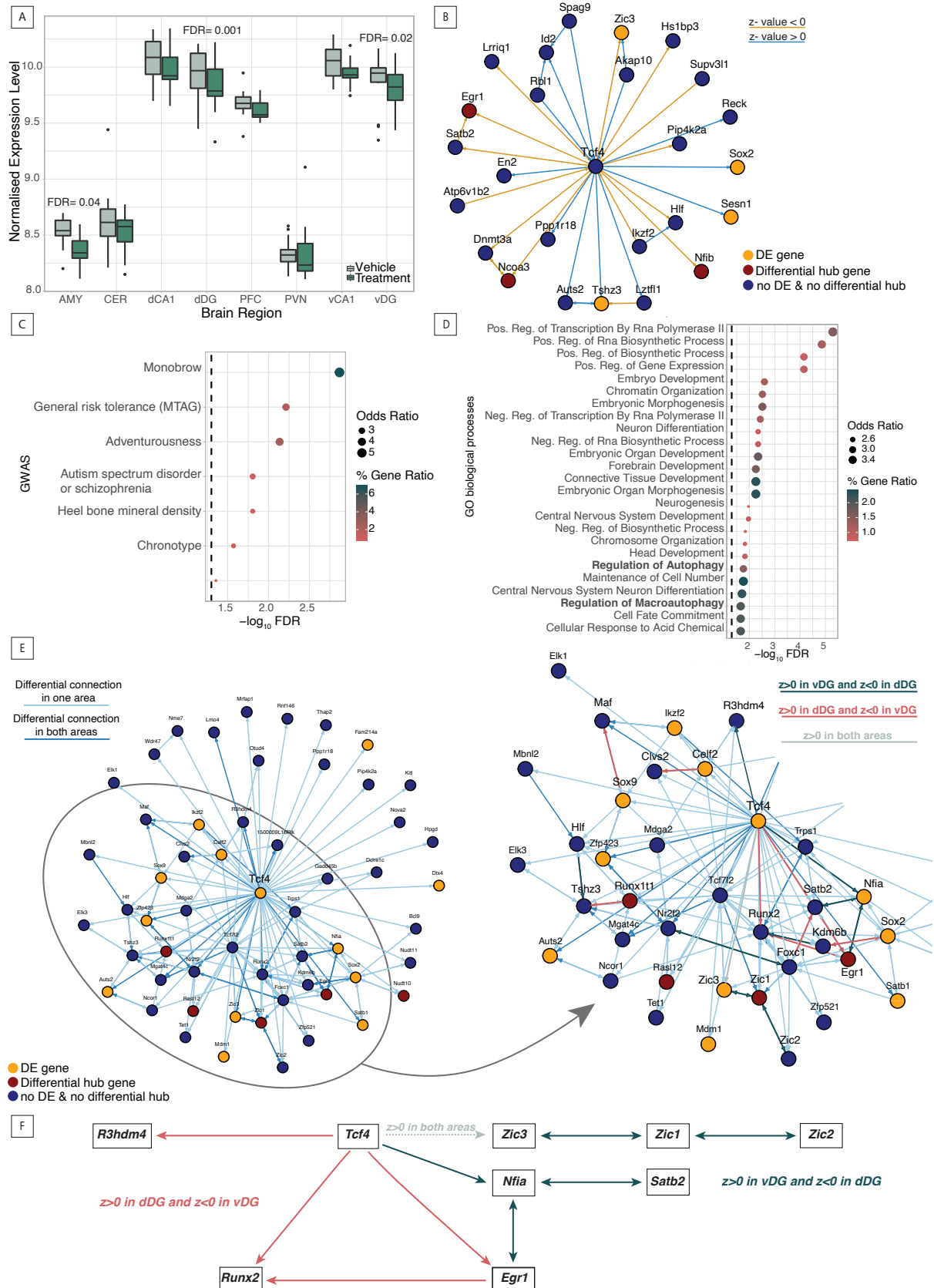


**Figure 5: DiffBrainNet can support exploring network changes related to candidate genes: the case of *Tcf4*.** (A) *Tcf4* is differentially expressed in the ventral and dorsal dentate gyrus (v/dDG) and in the AMY after 10mg/kg intraperitoneal dexamethasone treatment for 4 hours. (B) *Tcf4* DN in PFC. (C) *Tcf4*

PFC DN is enriched for genes that carry SNPs associated with the GWAS traits schizophrenia, autism spectrum disorder or schizophrenia, adventureness and general risk tolerance among others. (D) GO biological processes enrichment analysis shows that members of the *Tcf4* PFC differential network are associated with development, neuronal differentiation, RNA biosynthetic processes and gene expression but also with regulation of autophagy (bold). (E) Differential network of *Tcf4* in both vDG and dDG (left). Zoom-in on a highly interconnected part of the DG *Tcf4* DN (right). Coloured with red are all the connections with a positive regulatory effect in dDG and a negative regulatory effect in vDG, coloured in black are all the connections with a negative regulatory effect in dDG and a positive in vDG and coloured in green is one of the connections that has a positive regulatory effect in both areas. (F) *Tcf4* molecular pathways that are co-regulated in an opposite manner in vDG and in dDG. *Tcf4* connections with the *Zic* transcripts and with *Satb2* and *Nfia* have a positive regulatory effect in vDG and a negative one in dDG whereas *Tcf4* connections with *Runx2*, *Egr1* and *R3hdm4* have a negative regulatory effect in vDG and a positive in dDG. (Enrichment analyses are done with at least 10% of the input genes having to overlap with the genes of the term.)

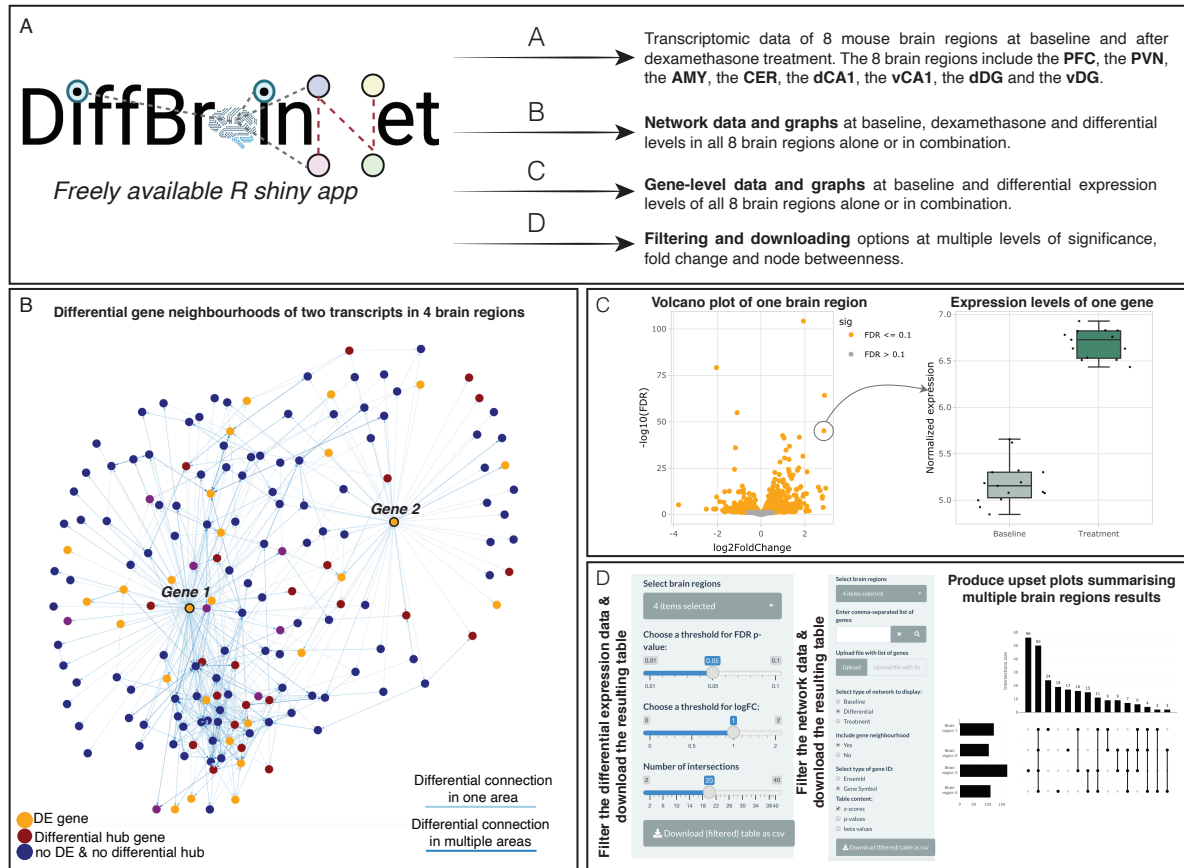


**Figure 6: DiffBrainNet: a resource of gene expression and network data for 8 mouse brain regions.** (A) DiffBrainNet includes gene expression and network data for 8 mouse brain regions at baseline, dexamethasone and differential levels. (B) DiffBrainNet provides network data for all 8 brain regions alone or in combination at baseline, treatment and differential levels. The data can be downloaded and plotted in the app. (C) DiffBrainNet provides gene expression data for all 8 brain regions. The data can be downloaded and plotted in the app. (D) The data both at the network- and the gene- levels can be downloaded using different thresholds of significance, fold change and node betweenness.